DOI: https://doi.org/10.37434/tpwj2022.09.05

CHEMICAL OVERLAP WELDING OF EPOXY VITREMERS AND THEIR NANOCOMPOSITES

A.V. Vashchuk, S.I. Motrunich, V.L. Demchenko, M.V. Iurzhenko, M.O. Kovalchuk, E.P. Mamunya

E.O. Paton Electric Welding Institute of the NASU
11 Kazymyr Malevych Str., 03150, Kyiv, Ukraine

ABSTRACT

In this work, the technology of chemical overlap welding of polymer materials based on epoxy resins (transparent film) and their nanocomposites with oxidized graphene (black film) was developed. The overlap welding of film materials with a thickness of 0.5 mm was carried out under the conditions of isothermal heating of 150 °C and pressure of the limiting plate. The selection of an effective welding mode was performed at different duration of welding: 30 and 60 min. Mechanical tests of the produced welded joints showed their strength at the level of the base material. Features of the structural organization of welded joints of composites were investigated by the method of wide-angle X-ray diffraction. The chemical structure of the material of welded joints was investigated by the Fourier transmission infrared spectroscopy. Modeling of stresses that occur in the specimens of welded joints was calculated using the values of the modulus of elasticity and the coefficient of linear expansion, experimentally found by the method of thermal mechanical analysis.

KEYWORDS: epoxy nanocomposites, oxidized graphene, vitremers, welded joints, chemical welding

INTRODUCTION

Development of shape-memory materials capable of reacting to environmental changes (temperature, power, electromagnetic field, solvent, humidity, etc.) and correcting their mechanical parameters (shape, position, deformation, etc.) for recovery to original state, is an important and relevant direction of development of construction machinery [1], structures deployed in space [2], artificial muscles [3], biomedical devices [4], sensors [5], and energy converters [6]. Solution of this problem is closely related to application of crosslinked polymers that is attributable to their high heat resistance, fixing ability and shape recovery rate. Fabrication of structures with shape-memory effect can be simplified by application of welding.

In the case of diffusion welding of dissimilar materials it is necessary to take into account the features of thermal impact on each of the welded polymer materials. The compatibility of material combinations is determined by the ratio of their coefficients of linear expansion (a_1/a_2). According to literature, the high strength of the joints produced by diffusion welding can be achieved only in such material combinations, for which $a_1/a_2 < 1.2$ [7], that essentially limits the applicability of welding.

Unlike diffusion welding which is due to the forces of intermolecular interaction in the joint zone, chemical welding takes place due to interaction of functional groups on the contacting surfaces with bond formation. Chemical welding of dissimilar materials into one part is rational for building more complex and multifunctional structures. In particular, joining polymer composites with discrete vitrification temperatures is one of the methods of producing thermosensitive shape-memory materials. Thus, the shape of each part is deformed and recovered at certain temperatures, independently one from another [8]. Another strategy of transformation of flat films into 3D-static structures is creation of two layers with further application of external stimuli (photo-, chemical or other treatment) [9, 10]. Active 3D-static structures were recently obtained by chemical welding of liquid-crystal elastomers based on epoxy resins and their composites with polydopamine (PDA) with their further two-directional tension [11]. So, the difference in the response to NIR-radiation (1.0 W/cm^2) led to specific 3D deformation in keeping with the pattern: the composite recovers its initial length, while the transparent film does not react to light and keeps its elongated shape, making the sample bend through 90° (Figure 1, *a*). Similarly, the linear pattern can be controlled by sample bending in the form of a circular arc (Figure 1, *b*), spiral (Figure 1, *c*), and claws (Figure 1, *d*). It should be noted that 2D-dynamic structures are required, which demonstrate automatic reversible change of shape, convenient for transportation and storage.

In this work a technology of chemical welding of transparent polymer films, based on epoxy resins and their composites with oxidized graphene, is proposed, features of structural organization of the produced welded joints were studied, and their mechanical and thermal properties were established.

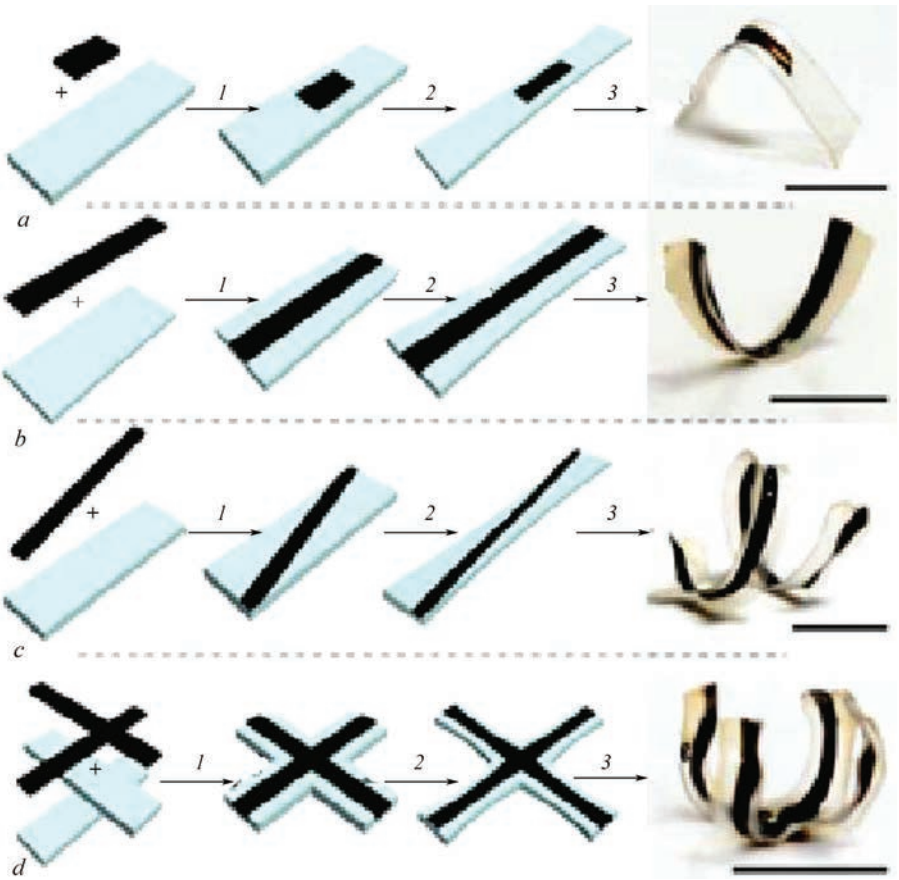

Figure 1. Schematic illustration of producing the welded joints and images of the respective 3D structures: composite film in the center (*a*), in the middle (*b*), diagonally (*c*) and crosswise (*d*)

MATERIALS AND EXPERIMENTAL PROCEDURES

Diglycyl ether of bisphenol A (4.4′-isopropylenediphenol diglycidyl ether, 2.2-bis[4-(glycidyloxy)phenyl]propane, DGEBA) with the following main characteristics: epoxy equivalent mass of 172–176, M = = 340.41 g/mole, ρ = 1.21 g/ml at 25 °C.

Trimethylolpropane tris(3-mercaptopropionate) (T_3M) with the following main characteristics: ≥95.0 %, $T_?$ = 220 °C/0.3 mm. Hg, n_{20D} = 1.518, M = = 398,56 g/mole, ρ = 1.16 g/ml at 25 °C.

Tin 2-ethylhexanoate (II) (tin octoate, tin salt of 2-ethylhexanoic acid, tin (II) 2-ethyhexanoate, $Sn(Oct)_2$) with the following main characteristics: 92.5–100.0 %, n_{20D} = 1.493, M = 405.12 g/mole, ρ = = 1.251 g/ml at 25 °C.

Oxidized graphene (OG). Nanoparticles of oxidized graphene consisted of blocks of 15–20 weakly bonded graphene layers with the following main characteristics: 4–10 % of oxidized edges (epoxy, carbonyl, hydroxyl, phenol groups) ρ = 1.8 g/cm^3. Detailed OG structure is still not understood, because of irregular application of the layers.

Transparent polymer films (polyDGEBA/T_3M)) were obtained by thermal solidification of DGEBA and T_3M at equal molar ratio of thiol and epoxy groups in the presence of 5.0 wt.% $Sn(Oct)_2$. Composite films (poly(DGEBA/T_3M)/OG) were obtained with OG addition to the produced mixture with filling concentration of 1.0 wt.% [12]. Mixture preparation was conducted in BAKU BK-2000 ultrasonic bath at 44 Hz frequency and 50 °C for 30 min. Mixture polymerization was performed under the conditions of step-like isothermal heating: 120, 150 °C/2 h. Thickness of the produced poly(DGEBA/T_3M) and poly(DGEBA/T_3M)/OG films was equal to 0.5 mm.

Testing for static uniaxial tension was conducted in keeping with ISO 527 standard in upgraded tensile testing machine 2054 R-5 fitted with 500N strain gauge. The samples were first cut out in the form of 60 mm long and 25 mm wide strips. Samples of film materials and welded joints were tested with the rate of 2 mm/min and temperature control (25 °C). Young's modulus E for each sample was calculated as the slope of σ–ε deformation curve between 0.25 and 0.5 % ε deformation. Elongation at rupture was determined as strain value at stress lowering to 10 % of the maximum strength value. Stresses at destruction for base material and samples of overlap joints were determined by the following formula:

$$\sigma_{br} = \frac{P_{br}}{S_c},$$

where σ_{br} are the breaking stresses, MPa; P_{br} are the breaking loads, N; S_c is the cross-sectional area in the fracture site, mm^2.

Morphological features of welded joint sections were studied using Versamet-2 microscope in the transmission mode in keeping with DSTU EN12814-5:2018. Recording of the obtained results was performed using a digital photocamera, with which the microscope is fitted.

Features of structural organization of poly(DGEBA/T_3M) and poly(DGEBA/T_3M)/OG films, as well as welded joints on their base were studied by the method of wide-angle radiography in XRD-7000 diffractometer (Shimadzu, Japan), where the X-ray optical scheme is made by the Debye-Scherrer method for passage of the primary beam through the studied sample, using CuK_α-radiation (λ = 1.54 A) and graphite monochromator. Investigations were performed by the method of automatic step-by-step scanning in the mode of 30 kV for 30 mA in the range of scanning angles (2θ) from 3.0 to 55° at exposure time of 5 s. Temperature of conducting the investigations was equal to 20 ± 2 °C. Mean distance between the molecular layers in amorphous polymers (*d*) was determined in keeping with Wulff–Bragg equation:

$$d = n\lambda(2 \sin \theta_m)^{-1},$$

where *n* is the ordinal number of the diffraction maximum (equal to a unity in studies of all the polymer types, as the structure of macromolecular compounds is of a relaxation nature); λ is the wave length of the characteristic X-ray radiation (λ = 1.54 A for CuK_α radiation), θ_m is the angular position of the diffraction maximum on scattering profile.

Chemical structure of the welded joints was studied by Fourier transmission infrared spectroscopy (FTIR), using Tensor 37 spectrometer of Bruker Company in the frequency range of 4000–600 cm^{-1}. For each spectrum 32 sequential scans with the resolution of 4 cm^{-1} were averaged. Intensity of absorption band with the maximum at 1607 cm^{-1}, which corresponds to phenyl group oscillations, was used as the internal standard.

Additional studies of the stressed-strained state of samples of base material (poly(DGEBA/T_3M) and poly(DGEBA/T_3M)/OG) and welded joints, were performed to assess the possible strains and stresses at sample heating. They were conducted using the ANSYS19.1 finite element analysis software. Modelling was performed at heating the samples from 40 to 100 °C. Experimentally established values of the modulus of elasticity and coefficient of linear expansion, obtained by the method of thermal mechanical analysis, were taken as the initial data for SSS calculation. Sample model of 60×10×0.5 mm size was broken down into a simple hexagonal finite-element mesh with element size of 0.25 mm.

EXPERIMENTAL PART AND DISCUSSION

Chemical overlap welding of (poly(DGEBA/T_3M) and poly(DGEBA/T_3M)/OG) was conducted by the thermomechanical method under the conditions of isothermal heating at 150 °C and pressure of the limiting plate, coated by antiadhesive film in MTS651.06E-04 Environmental Chamber (USA). Effective welding mode was selected on the base of the change of welding process duration. Two soaking scenarios were considered: 30 and 60 min. Scheme of overlap welded joint formation is shown in Figure 2, *a*. Energy supply into the joint zone by thermal heating ensured formation of 1.0 mm thick joint. Primary control of the joint quality by visual examination showed absence of defects, namely change of colour, OG pressing outside, as well as traces of burns-through, pores and cavities (Figure 2, *b*). It should be noted that no transition of (poly(DGEBA/T_3M) and poly(DGEBA/T_3M)/OG) into the plastic state took place during welding that is confirmed by the stability of their dimensions and absence of deformations after the joint formation (Figure 2, *b*).

A complex of tests and investigations was conducted for assessment of physico-mechanical properties of the produced (poly(DGEBA/T_3M) and poly(DGEBA/T_3M)/OG) films, as well as their overlap welded joints. It was found that destruction of welded joints produced during 30 min, runs through the weld, at

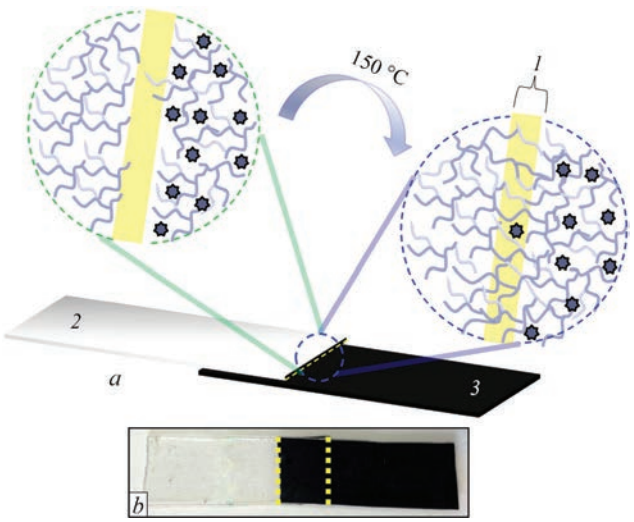

Figure 2. Schematic image of material structure recovery in the weld zone during chemical welding (*a*): *1* — weld zone; *2* — transparent film; *3* — composite; *b* — appearance of the produced overlap welded joint

Strength of the produced films and their welded joints

Sample	Welding mode		σ_{fr}, MPa	Fracture
	T, °C	*t*, min		
Poly(DGEBA/T_3M)	–		18.1–19.9	–
Poly(DGEBA/T_3M)/OG	–		20.1–22.4	–
Welded joint	150	30	8.1–9.5	Weld
		60	12.1–13.5	Poly(DGEBA/T_3M) base material

8.1–9.5 MPa (Table). At the same time, at increase of welding duration to 60 min, welded joints fail through base material (poly(DGEBA/T_3M), beyond the welded joint. It should be noted that in this case welded joint σ_{fr} is on the level of that of (poly(DGEBA/T_3M) base material.

Conducted studies of the macrostructure of experimental welded joints revealed absence of any signs of the interphase (Figure 3). Thus, during chemical welding no formation of an independent continuous phase, which would differ by its properties from those of poly(DGEBA/T_3M) and poly(DGEBA/T_3M)/OG base materials, was observed.

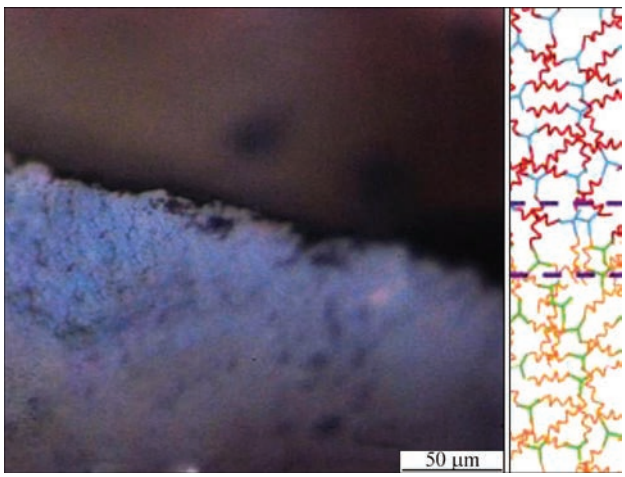

Figure 3. Optical photography of welded joint sections

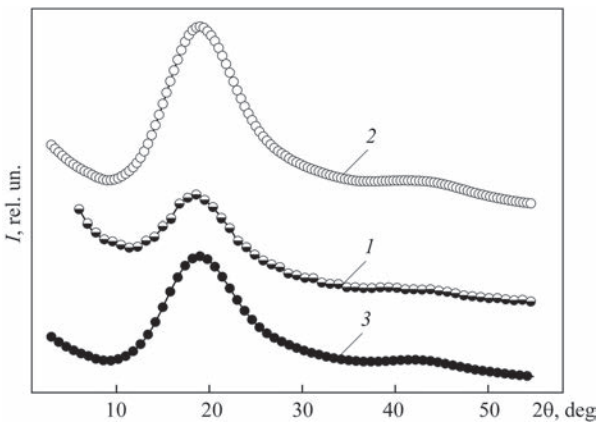

Figure 4. Wide-angle R-ray diffraction patterns of the welded joint: weld zone (*1*); poly(DGEBA/T_3M) (*2*); poly(DGEBA/T_3M)/OG (*3*)

Analysis of wide-angle X-ray diffraction patterns (Figure 4) showed that the welded joint is characterized only by short-range ordering during translation in space of fragments of internodal molecular links. This is evidenced by appearance on the diffraction pattern of one diffraction maximum of the diffuse type (amorphous halo) with $2\theta_m$ angular position close to 18.8°. However, mean distance between the layers of internodal molecular links in the welded joint is equal to 2.5 Å in keeping with Bragg's equation. At the same time, compared to base material of optically transparent (Figure 4, curve *2*) and composite films (Figure 4, curve *3*) no shifting of the diffraction maximum of diffuse type is recorded on the diffraction pattern of weld sample (Figure 4, curve *1*). It is indicative of the fact that the mean distance between the layers of molecular links does not change as a result of weld formation.

As was anticipated, 3441, 1735, 1607, 1509, 1244, 1032, 825 cm^{-1} absorption bands, typical for (poly(DGEBA/T_3M) base material were recorded in FTIR-spectra of the weld zone (Figure 5, curve *1*). Spectra of poly(DGEBA/T_3M) (Figure 5, curve *2*) and poly(DGEBA/T_3M)/OG (Figure 5, curve *3*) were used for comparison. It should be noted that absence of multiplet peaks in the frequency range of 500–400 cm^{-1} (characteristic for poly(DGEBA/T_3M)/OG) in the weld zone spectrum (Figure 5, curve *1*), confirms formation of the weld, which is identical to poly(DGEBA/T_3M) by its chemical structure.

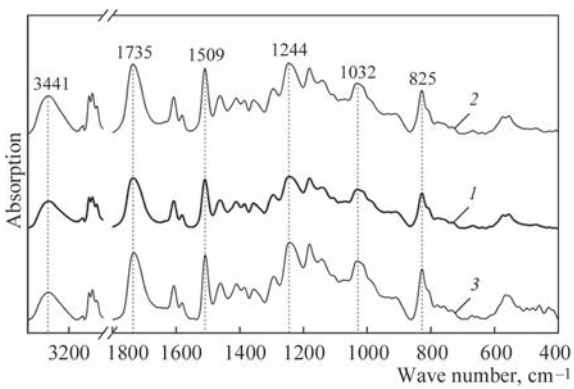

Figure 5. Typical FTIR spectra of the welded joint: weld zone (*1*); poly(DGEBA/T_3M) (*2*); poly(DGEBA/T_3M)/OG (*3*)

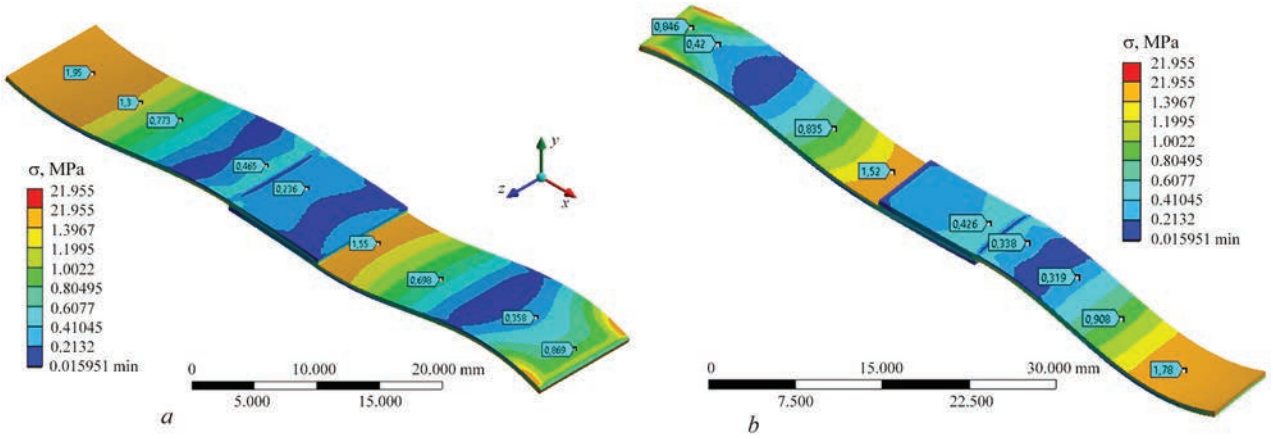

Figure 6. Stresses arising in the sample of overlap welded joint at calculation model I (poly(DGEBA/T_3M left part, poly(DGEBA/T_3M)/OG right part), at its heating from 40 to 100 °C (markers indicate stresses on the surface); *a* — top view; *b* — bottom view

Figures 6, 7 give the results of calculations of stresses arising in samples of overlap welded joints at their heating from 40 up to 100 °C (calculation model I and model II). It is shown that stresses arising in model I (poly(DGEBA/T_3M left part and poly(DGEBA/T_3M)/OG right part) are close to 1.95 MPa and in calculation model II (poly(DGEBA/T_3M left part), middle part with properties established for the weld zone, and poly(DGEBA/T_3M)/OG right part) they are equal to 2.36 MPa, at the same distance from the fixing point.

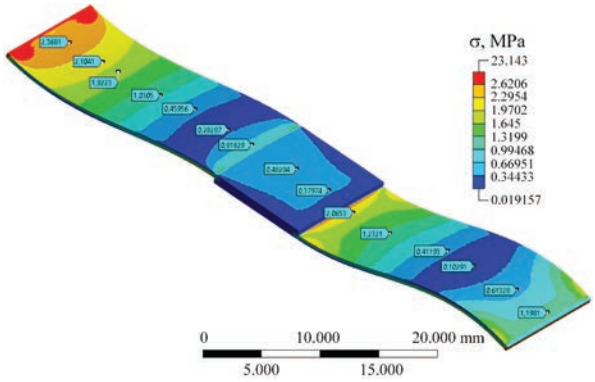

Figure 7. Stresses arising in the sample of overlap welded joint at calculation model II poly(DGEBA/T_3M left part), middle part with properties established for the weld zone, poly(DGEBA/T_3M)/OG right part)) at its heating from 40 up to 100 °C (markers indicate surface stresses)

CONCLUSIONS

Chemical welding of different materials into one part is rational for fabrication of more complex and multifunctional structures. This work gives the results of studies on development of the technology of chemical welding of transparent polymer films based on epoxy resins (transparent film) and their composites, filled with 1.0 wt.% of oxidized graphene (black film). Investigation showed that heating at 150 °C for 60 min is sufficient in general for formation of a sound welded joint. Visual examination of welds showed absence of the change of colour, pressing of oxidized graphene outside, or traces of burns-through, pores and cavities on the welded joint surface that ensures tightness and mechanical characteristics of the welded joint. Investigations of physico-mechanical properties of welded joints, produced at 60 min duration of welding showed that fracture occurs beyond the welded joint from the side of the transparent film material, and the strength limit is on the level of 12.1–13.5 MPa, respectively. Here, the overlap welded joint remains practically undamaged. Microstructural investigation of experimental welded joints showed that the images of the produced weld surface do not reflect formation of independent continuous interphase. FTIR spectral studies enabled establishing a full correlation between the spectra of the weld zone and transparent polymer film. It is found that during weld formation the mean distance between the layers of molecular links does not change that is confirmed by the results of wide-angle roentgenography. Finite element studies of the stress-strain state at higher temperatures in simple welded polymer products, using the obtained coefficients of linear expansion showed that the stresses arising in calculation model I, are close to 1.95 MPa, whereas in calculation model II they are equal to 2.36 MPa at the same distance from the fixing point.

Investigations were performed under the project of the Research Laboratories of Young Scientists of the NAS of Ukraine No. 11/01-2021(2) for conducting investigations in the priority directions of development of science and technology in 2020-2021 (Program No. 6541230).

REFERENCES

1. Zheng, Y. Dong, Y.H. Li (2018) Resilience and life-cycle performance of smart bridges with shape memory alloy (SMA)-cable-based bearings. *Construct. Build. Mater.*, **158**, 389–400.
2. Li, F., Liu, Y.J., Leng, J.S. (2019) Progress of shape memory polymers and their composites in aerospace applications. *Smart Mater. Struct.*, **28**, 103003.

3. Yuan, J.K., Neri, W., Zakri, C. et al. (2019) Shape memory nanocomposite fibers for untethered high-energy microengines. *Science*, **365**, 155–158.
4. Shin, Y.C., Lee, J.B., Kim, D.H. et al. (2019) Development of a shape-memory tube to prevent vascular stenosis. *Advanced Materials*, **31**, 1904476.
5. Li, Z., Qi, X.M., Xu, L. et al. (2020) A self-repairing, large linear working range shape memory carbon nanotubes/ethylene vinyl acetate fiber strain sensor for human movement monitoring. ACS Appl. Mater. *Interfaces*, 37(**12**), 42179–42192.
6. Xu, W., Wong, M.C., Guo, Q.Y. et al. (2019) Healable and shape-memory dual functional polymers for reliable and multipurpose mechanical energy harvesting devices. *J. Mater. Chem.*, **7**, 16267–16276.
7. Volkov, S.S. (2001) *Welding and adhesive bonding of polymer materials*. Moscow, Khimiya [in Russian].
8. Ji, F., Liu, X., Sheng, D., Yang, Y. (2020) Epoxy-vitrimer composites based on exchangeable aromatic disulfide bonds: Reprocessibility, adhesive, multishape memory effect. *Polymer*, **197**, 122514.
9. Na, J.H., Evans, A.A., Bae, J. et al. (2015) Programming reversibly self-folding origami with micropatterned photocrosslinkable polymer trilayers. *Advanced Materials*, **27**, 79–85.
10. Silverberg, J.L., Evans, A.A., McLeod, L. et al. (2014) Using origami design principles to fold reprogrammable mechanical metamaterials. *Science*, **345**, 647–650.
11. Li, Z., Yang, Y., Wang, Z. et al. (2017) Polydopamine nanoparticles doped in liquid crystal elastomers for producing dynamic 3D structures. *J. of Mater. Chem. A*, **5**, 6740–6746.
12. Vashchuk, A.V., Motrunich, S.I., Demchenko, V.L., Iurzhenko, M.V. (2022) Chemical welding of nanocomposites based on epoxy and oxidized graphene. *Avtomatychne Zvaryuvannya*, **4,** 50–53. DOI: https://doi.org/10.37434/as2022.04.07

ORCID
A.V. Vashchuk: 0000–0002–4524–4311,
S.I. Motrunich: 0000–0002–8841–8609,
V.L. Demchenko: 0000–0001–9146–8984,
M.V. Iurzhenko: 0000–0002–5535–731X,
M.O. Kovalchuk: 0000–0003–2161–643X,
E.P. Mamunya: 0000–0003–3855–2786

CONFLICT OF INTEREST
The Authors declare no conflict of interest

CORRESPONDING AUTHOR
M.V. Iurzhenko
E.O. Paton Electric Welding Institute of the NASU
11 Kazymyr Malevych Str., 03150, Kyiv, Ukraine.
E-mail: 4chewip@gmail.com

SUGGESTED CITATION
A.V. Vashchuk, S.I. Motrunich, V.L. Demchenko, M.V. Iurzhenko, M.O. Kovalchuk, E.P. Mamunya (2022) Chemical overlap welding of epoxy vitremers and their nanocomposites. *The Paton Welding J.*, **9**, 27–32.

JOURNAL HOME PAGE
https://pwj.com.ua/en

Received: 11.05.2022
Accepted: 11.11.2022